Theoretical study on the reactions of C2H5 with CnH2n+1OH (n = 1 - 4): Predicted rate constants and branching ratios

Trong-Nghia Nguyen
Hanoi University of Technology: Hanoi University of Science and Technology
Vu Anh Tuan
Hanoi University of Technology: Hanoi University of Science and Technology
Phung Thi Viet Bac
Vietnam National University Hanoi
Le Phuoc Anh
Vietnam National University Hanoi
Hue Minh Thi Nguyen (hue.nguyen@hnue.edu.vn)
Hanoi National University of Education https://orcid.org/0000-0001-6373-4691

Research Article

Keywords: C2H5, CnH2n+1OH (n=1-4), B3LYP, CCSD(T), H-abstraction, Rate constants

Posted Date: February 17th, 2022

DOI: https://doi.org/10.21203/rs.3.rs-1224120/v1

Abstract

The mechanisms of the reactions of C_2H_5 with $C_nH_{2n+1}OH$ (n = 1-4) have been investigated by CCSD(T)//B3LYP/6-311++G(3df,2p) for n = 1 - 3 and CCSD(T)//B3LYP/6-311+G(d,p) for n = 4. Our chemical quantum results show that the C_2H_5 + CH_3OH reaction can take place via H-abstraction or substitution channels. The former is the major channel with barrier energies of 13.0 and 14.4 kcal/mol while the latter has to pass over much higher barriers of 42.2 – 52.3 kcal/mol. Similarly, the C_2H_5 + $C_nH_{2n+1}OH$ (n = 2 - 4) reactions can mainly occur via H-abstraction channels with barrier energies of 10.4 - 16.4 kcal/mol. The b-H abstraction channel has the lowest barrier energy (11.7 kcal/mol) for t-C_4H_9OH while o/a-H abstraction channels have the lowest barrier energies (10.4 - 13.0 kcal/mol) for the others. The rate constants and product branching ratios for individual channels as well as total rate constants have been calculated for the temperature range 300-2500 K by TST theory with Eckart tunneling corrections. The optimized geometries of the related species and predicted heats of reactions agree well with available data.

1. Introduction

Alcohol fuels ($C_nH_{2n+1}OH$, n = 1-4) are recognized as the most promising renewable energy resources [1–9]. Methanol (CH_3OH) can be used in an internal engine via combustion or in a fuel cell. Ethanol (C_2H_5OH) is widely used; a large amount of ethanol is used in gasoline engines as an engine fuel such as E10 (i.e., a fuel blend of 10% C_2H_5OH and 90% gasoline), E15 (15% C_2H_5OH), E85 (85% C_2H_5OH), etc. n-Propanol (n-C_3H_7OH) and isopropanol (i-C_3H_7OH) are potential fuel additives. n-Propanol has a higher heating value than ethanol; isopropanol can readily be used as a fuel for existing engines. Butanols (n/i/s/t-C_4H_9OH) may be second-generation biofuel potential biofuels because they do not suffer from the drawbacks as ethanol does. The favorable characteristics of $C_nH_{2n+1}OH$ (n = 1-4) have led to an increasing number of studies investigating theirs use as a transportation fuel. Specifically, there are many papers concerned $C_nH_{2n+1}OH$ (n = 1-4) such as determining the structure of the molecules, vibrational frequencies, and heats of formation [10–12]; both experimental and theoretical papers concerning thermal decompositions of $C_nH_{2n+1}OH$ (n = 1-4) at high-temperatures in the internal engines via combustion [13–19], or their reactions with various atoms and radicals existed in combustion gas, such as H, OH, CH_3, etc [20–31]. The experimental studies by different techniques report their branching ratio and total rate constants at some specific conditions while the theoretical studies proposed the mechanisms and kinetics results at wide-range conditions, especially experimental difficulty in evaluating the branching fractions mainly arises from the contributions of the secondary reactions. Theoretically, the reactions can occur by various mechanisms including H- abstraction, insertion, and substitution reactions. For example, in the reactions of C_2H_5OH with CH_3 radical, Lin et al. [21] proposed that the methyl radical can abstract H atoms in the OH, CH_2, and CH_3 groups and substitute OH, CH_3 groups in the $C_nH_{2n+1}OH$ (n = 1-4) molecule. Using the quantum calculations at G2M level of theory, they concluded that the H abstraction channels are more favored than the latter. Based on the predicted potential energy

surface, they calculate rate constants and branching ratios for the H-abstraction reactions; their kinetics results are close to the available experiment.

Besides, ethyl radical (C_2H_5) is another important free radical in combustion and atmospheric and environmental chemistry [32–34]. Ethyl radical can be formed in the oxidation of natural gas which composes mostly of methane and ethane; for example, ethane can react with O_2 giving C_2H_5 as [33]: $C_2H_6 + O_2 \rightarrow C_2H_5 + HO_2$. It can also be generated when a large hydrocarbon radical decomposes into smaller radicals including ethyl and methyl radicals. C_2H_5 radical is considered as the simplest alkane radicals which can show oxidation features of big alkane radicals [27]. Therefore, its reactions have been attracted much interest, both experimental and theoretical such as reactions of C_2H_5 with O_2, HO_2, NCO, etc. [34–38].

However, the reactions of C_2H_5 with $C_nH_{2n+1}OH$ (n = 1-4) in combustion gas and atmosphere have not been elucidated yet in both mechanisms and kinetics. The present work aims are to elucidate the mechanism for the title reaction through a comprehensive and accurate quantum chemical calculation and to predict the kinetics of individual product channels employing transition state theory with appropriate quantum-mechanical tunneling corrections for combustion applications.

2. Computation Methods

All structures involved the $C_2H_5 + C_nH_{2n+1}OH$ (n = 1 - 4) reactions have been fully optimized by the DFT-B3LYP method [39, 40] excluding the transition state TS39 (see later) along with 6-311++G(3df,2p) and 6-311+G(d,p) basis sets for n = 1 - 3 and n = 4, respectively. Vibrational frequencies predicted at the same level of theory as the optimizations have been used for the rate constant calculations as well as zero-point energy (ZPE) corrections. They have also been employed for the determination of the optimized structures, in which the reactants (C_2H_5 and $C_nH_{2n+1}OH$ (n = 1 - 4)) and products possessed all positive vibrational frequencies, whereas each transition state (TS1-TS39) has only one imaginary frequency. To get more reliable energies for all the species, we performed higher-level single-point energy calculations with the CCSD(T) method [41, 42] and the same basis sets based on the B3LYP optimized geometries. The total energy of a species is the sum of the corresponding single-point energy by the CCSD(T) method with the ZPE corrections. All the ab initio calculations have been performed using the Gaussian 09 collection of programs [43].

The rate constants for individual channels of the title reactions have been calculated using the transition state theory (TST) [44] including Eckart tunneling effects [45] in the temperature range of 300 - 2500 K. In the TST calculations, the k^{TST} for each channel has been estimated as follows:

$$k^{TST} = \sigma \frac{k_B T}{h} \frac{Q_{TS}}{N_A Q_A Q_B} \exp\left[-\frac{E_{TS} - E_{A+B}}{k_B T}\right]$$

Where E_{TS} and E_{A+B} are potential energies of the TS (transition state) and A+B (reactants); Q_A, Q_B, and Q_{TS} are partition functions of the A, B, and TS; σ, k_B, T, h, and N_A are symmetry number, Boltzmann's constant, the temperature, the Planck's constant, and Avogadro's number, respectively. All the kinetics calculations have been performed with the Multiwell code [46]; the rate constants for individual channels as well as total reactions have been used to fit a modified Arrhenius equation for and presented in Tables 2 and S1 in the electronic supporting information (ESI).

Table 2
Arrhenius parameters [$k(T)= AT^n e^{-E/RT}$] for the C_2H_5 + $C_nH_{2n+1}OH$ (n = 1, 2) reactions.

Reactions	A	n	E	T – range (K)
CH_3OH				
$C_2H_5 + CH_3OH \rightarrow CH_3O + C_2H_6$	$7.37 \cdot 10^{36}$	7.07	-2915.1	300 - 600
$C_2H_5 + CH_3OH \rightarrow CH_3O + C_2H_6$	$1.93 \cdot 10^{24}$	3.51	-5084.1	600 - 2500
$C_2H_5 + CH_3OH \rightarrow CH_2OH + C_2H_6$	$7.58 \cdot 10^{50}$	11.57	-1101.3	300 - 600
$C_2H_5 + CH_3OH \rightarrow CH_2OH + C_2H_6$	$1.35 \cdot 10^{25}$	3.97	-5503.5	600 - 2500
$C_2H_5 + CH_3OH \rightarrow$ Products	$1.31 \cdot 10^{40}$	8.69	-2264.4	300 - 600
$C_2H_5 + CH_3OH \rightarrow$ Products	$2.11 \cdot 10^{25}$	3.94	-5105.8	600 - 2500
C_2H_5OH				
$C_2H_5 + C_2H_5OH \rightarrow C_2H_5O + C_2H_6$	$1.33 \cdot 10^{33}$	6.44	-3182.3	300 - 600
$C_2H_5 + C_2H_5OH \rightarrow C_2H_5O + C_2H_6$	$1.33 \cdot 10^{23}$	3.31	-4987.8	600 - 2500
$C_2H_5 + C_2H_5OH \rightarrow CH_3CHOH + C_2H_6$	$4.20 \cdot 10^{46}$	10.36	-1073.8	300 - 600
$C_2H_5 + C_2H_5OH \rightarrow CH_3CHOH + C_2H_6$	$4.07 \cdot 10^{24}$	3.50	-5151.5	600 - 2500
$C_2H_5 + C_2H_5OH \rightarrow CH_2CH_2OH + C_2H_6$	$3.98 \cdot 10^{47}$	10.76	-2842.3	300 - 600
$C_2H_5 + C_2H_5OH \rightarrow CH_2CH_2OH + C_2H_6$	$1.42 \cdot 10^{24}$	3.69	-6935.4	600 - 2500
$C_2H_5 + C_2H_5OH \rightarrow$ Products	$4.15 \cdot 10^{41}$	8.91	-1908.1	300 - 600
$C_2H_5 + C_2H_5OH \rightarrow$ Products	$6.52 \cdot 10^{25}$	3.84	-4845.1	600 - 250

3. Results And Discussion

3.1. Potential energy surfaces and reaction mechanisms

The geometries of the reactants and products for the C_2H_5 and n-$C_nH_{2n+1}OH$ (n = 1 - 4) reactions are shown in Figs. 1 (for n = 1, 2) and S1 (for n = 3, 4) in the ESI; those of the transition states are in Figs. 2 (for n = 1, 2) and S2 (for n = 3, 4). The potential energy surfaces for the title reactions are shown in Figs. 3 (for n = 1, 2) and S3 (for n = 3, 4) in the ESI, and heats of reaction for the C_2H_5 + $C_nH_{2n+1}OH$ (n = 1, 2) reactions are shown in Table 1.

Table 1
Comparison of Heats of reaction for the C_2H_5 + $C_nH_{2n+1}OH$ (n = 1, 2) reactions calculated at the CCSD(T)//B3LYP /6-311++G(3df,2p) level of theory with available data [54–58].

Reactions	$\Delta_r H°_0$ (kcal/mol)		$\Delta_r H°_{298}$ (kcal/mol)	
	Predicted	Literature*	Predicted	Literature*
$CH_3OH + C_2H_5$				
PR1 ($CH_3O + C_2H_6$)	3.2	4.4 ± 1.1	2.7	4.1 ± 1.1
PR2 ($CH_2OH + C_2H_6$)	-4.6	-5.0 ± 0.8	-4.9	-5.0 ± 0.8
PR3 ($CH_3OC_2H_5 + H$)	17.7	19.3 ± 0.6	17.4	19.5 ± 0.6
PR4 ($C_2H_5OH + CH_3$)	-2.4	-2.1 ± 0.7	-2.4	-1.9 ± 0.7
PR5 ($C_3H_8 + OH$)	3.1	3.1 ± 0.7	2.8	3.1 ± 0.7
PR6 (n-$C_3H_7OH + H$)	9.8	10.3 ± 0.6	9.6	10.3 ± 0.6
$C_2H_5OH + C_2H_5$				
PR7 ($C_2H_5O + C_2H_6$)	3.0	4.0 ± 2.1	2.8	3.9 ± 2.1
PR8 ($CH_3CHOH + C_2H_6$)	-5.8	—	-6.1	—
PR9 ($CH_2CH_2OH + C_2H_6$)	1.5	—	1.5	—
PR10 ($C_2H_5OC_2H_5 + H$)	17.3	18.6 ± 1.1	17.3	19.4 ± 1.1
PR11 ($C_2H_5OH + C_2H_5$)	0.0	0.0	0.0	0.0
PR12 (n-$C_4H_{10} + OH$)	5.8	5.7 ± 1.3	5.7	6.1 ± 1.3
PR13 (s-$C_4H_9OH + H$)	8.0	—	7.9	—
PR14 (n-$C_4H_9OH + H$)	12.5	—	12.5	—
PR15 ($C_3H_8 + CH_2OH$)	-1.6	-1.9 ± 1.3	-1.9	-1.9 ± 1.3
PR16 (n-$C_3H_7OH + CH_3$)	0.6	1.0 ± 1.1	0.8	1.3 ± 1.1
*The experimental values employed in the calculations are obtained based on the heats of formation at 0K and 298K for the corresponding species from the literature [54–58].				

The reaction of C_2H_5 + CH_3OH:

The PES in Figure 1a reveals that the C_2H_5 radical can abstract H atoms in the OH and CH_3 groups giving PR1 ($CH_3O + C_2H_6$) and PR2 ($CH_2OH + C_2H_6$), or substitute atoms and groups such as H, OH, CH_3 in the CH_3OH molecule giving PR3 ($CH_3OC_2H_5$ + H) – PR6 (n-C_3H_7OH + H). The substitution channels should be very minor because of having significantly higher barrier energies of ~ 30 kcal/mol.

Formation of PR1 ($CH_3O + C_2H_6$) and PR2 ($CH_2OH + C_2H_6$):

These channels can occur from CH_3OH when the C_2H_5 radical abstracts H atoms in the OH, and CH_3 groups via TS1 (C_2H_5...H...OCH_3) and TS2 (C_2H_5...H...CH_2OH) giving PR1 ($CH_3O + C_2H_6$) and PR2 ($CH_2OH + C_2H_6$), respectively, as clearly shown in Fig. 1. The geometries of CH_3OH, C_2H_6, and CH_3O optimized at the B3LYP/6-311++G(3df,2p) level agree well with the experimental values (see Fig. 1). For example, the O-H, C-O, and C-H bond lengths of CH_3OH computed in this work are 0.960, 1.421, and 1.088 Å, which is in good agreement with the experimental value of 0.956, 1.427, and 1.096 Å, respectively [10]. For the transition states TS1 and TS2, there are no experimental results but their geometries agree well with the previous theoretical studies. For example, the length of the broken O…H bond in TS1 calculated in this work, 1.253 Å, is close to 1.2479 Å for the $CH_3 + CH_3OH$ reaction by Jodkowski et al.[25] The imaginary frequencies are 1524*i* cm^{-1} for TS1 and 1715*i* cm^{-1} for TS2 computed at the B3LYP/6-311++G(3df,2p) level corresponding migrations of the H atoms from O and C of the CH_3OH molecule to the C_2H_5 radical. The relative energies for TS1 and TS2 predicted at the CCSD(T)//B3LYP/6-311++G(3df,2p) level of theory in this work are 13.0 and 14.4 kcal/mol which are in good agreement with 13.6 and 14.0 kcal/mol, respectively, corresponding to the barrier energies for H-abstractions of the $CH_3 + CH_3OH$ reaction calculated at the G2 level of theory reported by Jodkowski et al. [25]. In addition, we have also compared the predicted heats of reaction ($\Delta_r H°$) for the channels with available experimental data at both 0 and 298 K (see Table 1). The heat of formation for each channel is evaluated with the heats of formation of CH_3OH (-190,12 ± 0,6 kJ/mol), C_2H_5, CH_3O (28,4 ± 2,1 kJ/mol), CH_2OH (-10,7 ± 0,7 kJ/mol) and C_2H_6 (-68,38 ± 0,4 kJ/mol) species from the available experimental data [54–57]. The heats of reaction for channels giving the PR1 and PR2 predicted at the CCSD(T)//B3LYP/6-311++G(3df,2p) level to be 3.2 and -4.6 kcal/mol at 0 K; 2.7 and -4.9 kcal/mol at 298 K, respectively. These values are in good agreement with the experimental values of 4.4 ± 1.1 and -5.0 ± 0.8 kcal/mol at 0 K and 4.1 ± 1.1 and -5.0 ± 0.8 kcal/mol at 298 K, respectively.

Formation of PR3 ($CH_3OC_2H_5$ + H), PR4 ($C_2H_5OH + CH_3$), PR5 ($C_3H_8 + OH$), and PR6 (n-C_3H_7OH + H):

The products can be formed when the C_2H_5 radical substitutes the H atoms, OH, and CH_3 groups in the CH_3OH molecule via TS3, TS4, TS5, and TS6, respectively (see Fig. 1a). The geometries of these transition states are also close to those in the previous studies. For example, the length of the breaking (C_2H_5…O) and forming (CH_3…O) bond lengths of TS4 in this work, 1.845 and 1.860 Å, are close to 1.847 and 1.862 Å for the $CH_3 + C_2H_5OH$ by Lin et al. [21]. Our predicted heats of reaction for channels giving the PR3, PR4, PR5 and PR6, 17.7, -2.4, 3.1 and 9.8 kcal/mol at 0 K; 17.4, -2.4, 2.8 and 9.6 kcal/mol at 298 K, respectively, are reasonable agreement with the experimental values of 19.3 ± 0.6, -2.1 ± 0.7, 3.1 ± 0.7

and 10.3 ± 0.6 kcal/mol at 0 K; 19.5 ± 0.6, -1.9 ± 0.7, 3.1 ± 0.7 and 10.3 ± 0.6 kcal/mol at 298 K, respectively (see Table 1). It is noticed that these barrier energies (TS3 – TS6) are much higher (> 27 kcal/mol) than those for the H-abstractions (TS1 and TS2); this picture agrees with the results for the CH_3 + C_2H_5OH reaction by Lin et al. [21]. It is obvious that the channels giving PR3 – PR6 should be kinetically unimportant because of having very high barrier energies at TS3 – TS6.

The reaction of C_2H_5 + C_2H_5OH:

Figure 1b reveals that the C_2H_5 radical can abstract H atoms in the OH, CH_2, and CH_3 groups giving PR7 (C_2H_5O + C_2H_6, 3.0 kcal/mol), PR8 (CH_3CHOH + C_2H_6, -5.5 kcal/mol), and PR9 (CH_2CH_2OH + C_2H_6, 1.5 kcal/mol) via transition states at TS7, TS8, and TS9, respectively. The geometries of the ethanol molecule and transition states predicted at the B3LYP/6-311++G(3df,2p) level of theory agree well with the previous studies (see Figures 1 and 2). For example, in the TS7 – TS9, the broken O…H, C…H (in CH_2 group), and C…H (in CH_3 group) are elongated by 31%, 21%, and 25% while the corresponding values for the CH_3 + C_2H_5OH reaction are 26%, 17%, and 22%, respectively by Lin et al. [21]. The relative energies of TS7 (13.0 kcal/mol), TS8 (12.6 kcal/mol), and TS8 (16.7 kcal/mol) are close to the corresponding values of 13.2, 12.0, and 16.0 kcal/mol for the CH_3 + C_2H_5OH reaction predicted at the G2M(RCC2) level of theory. It is noticed that among H- abstractions of the o-H (OH group), α-H (CH_2 group), and β-H (CH_3 group), the last channel has higher barrier energy of about 3.7 kcal/mol suggesting that this channel has a small contribution at the normal temperature. This picture is also in reasonable agreement with the result of Lin et al for the CH_3 + C_2H_5OH reaction [21]. In addition, the C_2H_5 radical can substitute H atom and OH, CH_3, and C_2H_5 groups in the C_2H_5OH molecule via transition states at TS10 – TS16 giving PR10 ($C_2H_5OC_2H_5$ + H) – PR16 (n-C_4H_9OH + CH_3). However, these substitution channels are unfavorable on account of the high barriers at the TS10 – TS16 (41.5 – 57.0 kcal/mol) (see Figure 3b).

The reaction of C_2H_5 + n/i-C_3H_7OH:

For the C_2H_5 + n-C_3H_7OH system, there are four reaction channels as clearly shown in Figure S2a: the C_2H_5 radical can abstract o-H (in the OH group), α-H (in the CH_2 group), β-H (in the CH_2 group) or γ-H (in the CH_3 group) giving PR17 (n-C_3H_7O + C_2H_6, 3.0 kcal/mol), PR18 (CH_3CH_2CHOH + C_2H_6, -5.4 kcal/mol), PR19 (CH_3CHCH_2OH + C_2H_6, -1.2 kcal/mol), and PR20 ($CH_2CH_2CH_2OH$ + C_2H_6, 0.4 kcal/mol) via transition states TS17, TS18, TS19, and TS20, respectively. Figure S2a also shows that among the energy barriers, the value of TS18 corresponding to the α-H abstraction is lowest with an activation energy of 12.1 kcal/mol compared to 12.9 kcal/mol at TS18 (for o-H abstraction), 14.0 kcal/mol at TS19 (for γ-H abstraction) and 15.8 kcal/mol at TS20 (for δ-H abstraction) suggesting the α-H abstraction is the major channel for the C_2H_5 + n-C_3H_7OH reaction. For C_2H_5 + i-C_3H_7OH reaction, the C_2H_5 radical can abstract o-H (in the OH group), α-H (in the CH group), β-H (in the CH_3 groups) giving PR21 (i-C_3H_7O + C_2H_6, 4.8 kcal/mol), PR22 ($CH_3C(CH_3)OH$ + C_2H_6, -6.6 kcal/mol) and PR23 ($CH_2CH(CH_3)OH$ + C_2H_6, 1.9 kcal/mol) via TS21, TS22, and TS23, respectively (see Figure S2b). It is noticed that the energy barrier for the α-H

abstraction (TS21) is only 10.4 kcal/mol which is the lowest energy barrier among the C_2H_5 + $C_nH_{2n+1}OH$ (n = 1 - 4) reactions because of the effect of the two CH_3 groups and OH group in i-C_3H_7OH molecule. This barrier is also lower ~ 2 – 6 kcal/mol than the others at TS22 (12.7 kcal/mol) and TS23 (16.4 kcal/mol) suggesting that the α-H abstraction channel should be the major channel in the C_2H_5 + i-C_3H_7OH reaction.

The reaction of C_2H_5 + n/i/s/t-C_4H_9OH:

For the C_2H_5 + n/i/s/t-C_4H_9OH systems, we calculate with a smaller basic set at the CCSD(T)//B3LYP/6-311+G(d,p) level of theory because of their large systems. For the C_2H_5 + t-C_4H_9OH reaction, Figure S2 shows that there are two channels including o-H and β-H abstractions in which the former has lower barrier energy of 12.8 (TS38) than that of 15.4 kcal/mol (TS39) for the latter. The barrier energy for o-H abstraction channel (12.8 kcal/mol) for the C_2H_5 + t-C_4H_9OH reaction predicted at the CCSD(T)//B3LYP/6-311+G(d,p) level of theory agree well with those of 12.9 and 13.0 kcal/mol for the C_2H_5 + $C_nH_{2n+1}OH$ (n = 2,3) reactions, respectively, predicted at the CCSD(T)//B3LYP/6-311++G (3df,2p) level of theory. The barrier energy of the H abstraction from the CH_3 group for the t-C_4H_9OH (TS39, 15.4 kcal/mol) also agrees well with those for n/i/s-C_4H_9OH with the values of 15.6-16.0 kcal/mol (see Fig. 3S in the ESI). It is noticed that TS39 is the unique species in the title reactions optimized at the BHandHLYP/6-311+G(d,p) level because we cannot find it at the B3LYP/6-311+G(d,p) level of theory. Its relative energy, therefore, is calculated from energies of TS39, t-C_4H_9OH, and C_2H_5 species at the CCSD(T)//BHandHLYP/6-311+G(d,p) level. The C_2H_5 + i-C_4H_9OH reaction has four channels including o-H, α-H, β-H, and γ-H abstractions in which the lowest energy barrier is the β-H abstraction (TS31, 11.7 kcal/mol) because of the effect of the two CH_3 groups in the i-C_4H_9OH molecule. Energy barriers for the o-H, α-H, and γ-H abstraction channels in the C_2H_5 + i-C_4H_9OH reaction, 12.6, 12.3, and 15.6 kcal/mol at TS29, TS30, and TS32, respectively, also agree well with the corresponding values at 12.9, 12.1, and 15.8 kcal/mol for n-C_3H_7OH + C_2H_5 reaction as discussed above. For the reactions of the C_2H_5 radical with n/s-C_4H_9OH, Figure S2 shows that there are five channels in which the o-H and α-H abstraction channels have lowest the barrier energies. The o-H abstractions occur via TS24 and TS33 lying 12.6 above the reactants for both n-C_4H_9OH and s-C_4H_9OH, respectively. The α-H abstractions are slightly lower than those for o-H abstractions with relative energies of 11.9 and 11.0 kcal/mol for n-C_4H_9OH and s-C_4H_9OH, respectively while the values for the other channels are 13.8 – 16.0 kcal/mol. It is clear that the difference between the barrier energies is small suggesting that all of the channels can contribute at high temperatures.

3.2. Rate constant calculations

Based on the PES and molecular parameters of all the related species in the C_2H_5 + $C_nH_{2n+1}OH$ (n = 1 - 4) reactions calculated by both the CCSD(T) and B3LYP methods as discussed above, we calculated the individual and total rate constants with TST considering Eckart tunneling effect in the temperature range of 300 – 2500 K; the results are presented in Fig. 4 for the C_2H_5 + $C_nH_{2n+1}OH$ (n = 1, 2) reactions and in

Fig. S4 in the ESI for the C_2H_5 + $C_nH_{2n+1}OH$ (n = 3, 4) reactions. The branching ratios calculated from the individual and total rate constants for each channel are presented in Figs. 5 and S5 for the reactions of C_2H_5 with $C_nH_{2n+1}OH$ (n = 1, 2) and $C_nH_{2n+1}OH$ (n = 3, 4), respectively.

It can be seen in Fig. 4 and S4 that all the rate constants have positive temperature dependence reflecting the fact that each channel has prominent and distinct barrier energy. For the C_2H_5 + CH_3OH reaction, the rate constants for the substitution reactions via TS3 – TS6 is very much smaller than those for H-abstraction via TS1 and TS2 for all the considered temperatures (see Figure 5a). For example, the values for the channels via TS1 and TS3 are $4.06 \cdot 10^{-16}$ and $1.70 \cdot 10^{-24}$ (cm^3 $molecule^{-1}$ s^{-1}) at 1000 K, respectively. Therefore, the branching ratios for the channels via TS3 – TS6 are very small with the highest value is only $\sim 4 \cdot 10^{-3}$ for the channel via TS4 at 2500 K. This is because the barrier energies for these channels are much higher (> 27 kcal/mol) than those for the H-abstraction channels as discussed above. As a result, the H-abstraction channels giving PR1 (CH_3O + C_2H_6) and PR2 (CH_2OH + C_2H_6) should be the major channels while the substitution channels giving PR3 – PR6 should be ignored in the C_2H_5 + CH_3OH reaction. Our kinetics results show that the branching ratios for PR1 and PR2 channels are not much different in the considered temperatures; the values for PR1 are from 0.62 at 300 K to 0.32 at 2500 K. The temperature dependence of the total rate constant for the C_2H_5 + CH_3OH reaction can be expressed, in terms of three-parameters fits of the form AT^n exp(-E/T), as follows:

$k(T) = 1.31 \times 10^{40}\ T^{8.69}$ exp(-2264.4 K/T) (T = 300 – 600 K)

$k(T) = 2.11 \times 10^{25}\ T^{3.94}$ exp(-5105.8 K/T) (T = 600 – 2500 K)

For the C_2H_5 + $C_nH_{2n+1}OH$ (n = 2 - 4) reactions, we did not calculate the rate constants for the substitution channels because of high barrier energies as discussed above. For the reaction of C_2H_5OH, the β-H abstraction channel via TS9 are about 2 orders lower than those for α-H and o-H abstraction channels via TS7 and TS8 at 300 K agreeing with the fact that the barrier energy at TS9 (16.7 kcal/mol) is higher than those at TS7 (13.0 kcal/mol) and TS8 (12.6 kcal/mol). However, the branching ratios for the three pair products PR7 (C_2H_5O + C_2H_6), PR8 (CH_3CHOH + C_2H_6), and PR9 (CH_2CH_2OH + C_2H_6, 1.5 kcal/mol) via TS7, TS8, and TS9 are almost the same at high temperatures; at 2500 K, the values for PR7, PR8, and PR9 are 0.31, 0.39, and 0.30, respectively. For the reactions of n/i-C_3H_7OH and n/s-C_4H_9OH, one can see that the α-H abstraction channels are dominant at 300 K due to the low barrier energies as discussed above. But their branching ratios decrease when temperature increases; all the products via H-abstraction channels, therefore, become competitive. For example, at 2500 K, for the reaction of n-C_3H_7OH, the branching ratios of o-H, α-H, β-H, and γ-H abstraction channels are 0.19, 0.36, 0.27, and 0.18, respectively. For the reaction of i-C_4H_9OH, Fig. 5S show that the β-H abstraction channel is dominated at all the considered temperature range of 300-2500K due to its lowest barrier energy. Its branching ratio also decreases when temperature increases but it is still highest at 2500K with the value of 0.431. For the reactions of t-C_4H_9OH, there are two H abstraction channels at o-H and β-H; the first channel is dominated at 300K with the branching ratio value of 0.761 but decreases to 0.297 at 2500K.

For convenient modeling applications, the temperature dependence of the individual reaction rate constants for the title reactions given in terms of three parameters fits the form $AT^n exp(-E/T)$ expressions in the temperature range of 300 - 1000 K are summarized in Table II.

4. Conclusions

Mechanism and kinetics for the reactions of C_2H_5 + $C_nH_{2n+1}OH$ (n = 1 - 4) have been investigated for the first time by both quantum-chemical and TST calculations. The quantum-chemical results show that the tile reactions can mainly undergo H-abstraction with barrier energies of 10.4 - 16.4 kcal/mol. The rate constants and product branching ratios have been calculated for the temperature range of 300-2500 K. The predicted rate constants and branching ratios for the H-abstraction reactions have been calculated using the transition state theory with quantum-mechanical tunneling corrections for the temperature range. The kinetics results show that all the rate constants increase when temperature increases. For the C_2H_5 + i-C_4H_9OH reaction, the β-H abstraction channels via barrier energy of 11.7 kcal/mol giving $(CH_3)_2CCH_2OH$ + C_2H_6 are dominated at all the considered temperatures. For the C_2H_5 + t-C_4H_9OH reaction, there are two channels including o-H and β-H abstractions via barrier energy of 12.8 and 15.4 kcal/mol, respectively, in which the latter is more favor at high temperatures (> 1500K). For others, the α-H abstraction channels are dominated at temperatures below 500K but all of the products via H abstraction channels can contribute at a high-temperature range of 2000–2500K. The temperature dependence of the individual reaction rate constants for the title reactions is provided for further modeling applications. Our geometries and heats of reaction are in good agreement with available experimental data.

Declarations

Acknowledgements

This research is funded by Vietnam National Foundation for Science and Technology Development (NAFOSTED) under grant number 104.06-2018.33.

Author Contributions

All authors contributed to the conceptualization and realization of the study. Trong-Nghia Nguyen carried out the computations and wrote the first draft. Writing review and editing by Hue Minh Thi Nguyen and revision was done by her with help of the other authors. All authors have read and agree to the published version of the manuscript.

Supplementary Information

The supplement related to this article is available online and contains extended information on the calculations.

Conflict of Interest

The authors declare no conflict of interest.

References

1. Aronowitz D, Naegeli DW, Glassman I (1977) J Phys Chem 81:2555. https://doi.org/10.1021/j100540a037
2. Wu CW, Lee YP, Xu S, Lin MC (2007) J Phys Chem A 111:6693. doi: 10.1021/jp068977z
3. Poh CH, Poh CK (2017) Adv Aerosp Sci Tech 2:23. doi: 10.4236/aast.2017.23003
4. Qian Y, Guo J, Zhang Y, Tao W, Lu X (2018) Appl Therm Eng 144:126. https://doi.org/10.1016/j.applthermaleng.2018.08.044
5. Mertens LA, Manion JA (2021) Int J Chem Kinet 53:95. DOI: 10.1002/kin.21428
6. Kumar K, Zhang Y, Sung CJ, Pitz WJ (2015) Combust Flame 162:2466. https://doi.org/10.1016/j.combustflame.2015.02.014
7. Rosado-Reyes CM, Tsang W (2013) J Phys Chem A 117:10170. https://doi.org/10.1021/jp404877t
8. Cai J, Yuan W, Ye L, Cheng Z, Wang Y, Zhang L, Zhang F, Li Y, Qi F (2013) *Combust. Flame 160*, 1939
9. http://dx.doi.org/10.1016/j.combustflame.2013.04.010
10. Heyne JS, Dooley S, Dryer FL (2013) J Phys Chem A 117:8997. https://doi.org/10.1063/1.1742240
11. Venkateswarlu P, Gordy W (1955) J Chem Phys 23:1200. https://doi.org/10.1063/1.1742240
12. Shimanouchi T Tables of molecular vibrational frequencies. Consolidated Volume 1, NSRDS NBS-39
13. Coussan S, Bouteiller Y, Perchard JP, Zheng WQ (1998) J Phys Chem A 102:5789. https://doi.org/10.1021/jp9805961
14. Aronowitz D, Naegeli DW, Glassman I (1977) J Phys Chem 81:2555. https://doi.org/10.1021/j100540a037
15. Wu CW, Matsui H, Wang NS, Lin MC (2011) J Phys Chem A 115:8086. https://doi.org/10.1021/jp202001q
16. Barnard JA, Hughes HWD (1960) Trans Faraday Soc 56:64. https://doi.org/10.1039/TF9605600064
17. J. A. Barnard, The pyrolysis of isopropanol.Trans. Faraday Soc.5672–79. https://doi.org/10.1039/TF9605600072
18. Barnard JA (1957) Trans Faraday Soc 53:1423. https://doi.org/10.1039/TF9575301423
19. Gu X, Huang Z, Wu S, Li Q (2010) *Combust. Flame 157*, 2318. https://doi.org/10.1016/j.combustflame.2010.07.003
20. Grana R, Frassoldati A, Faravelli T, Niemann U, Ranzi E, Seiser R, Cattolica R, Seshadri K (2010) Combust Flame 157:2137. https://doi.org/10.1021/jp806464p
21. Lee PF, Matsui H, Xu DW, Wang NS (2013) J Phys Chem A 117:525. https://doi.org/10.1021/jp309745p
22. Xu ZF, Park J, Lin MC (2004) J Chem Phys 120:6593. https://doi.org/10.1063/1.1650832

23. Moss JT, Berkowitz AM, Oehlschlaeger MA, Biet J, Warth V, Glaude PA, Battin-Leclerc F (2008) J Phys Chem A 112:10843. https://doi.org/10.1021/jp806464p
24. Heyne JS, Dooley S, Dryer FL (2013) J Phys Chem A 117:8997. https://doi.org/10.1021/jp404143f
25. Lendvay G, Berces T, Marta F (1997) J Phys Chem A 101:1588. https://doi.org/10.1021/jp963188a
26. Jodkowski JT, Rayez MT, Rayez JC, Bérces T, Dóbé. S (1999) J Phys Chem A 103:3750. https://doi.org/10.1021/jp984367q
27. Xu S, Lin MC (2007) *Proc. Combust. Inst. 31*, 159. https://doi.org/10.1016/j.proci.2006.07.132
28. Galano A, Alvarez-Idaboy JR, Bravo-Perez G, Ruiz-Santoyo ME (2002) Phys Chem Chem Phys 4:4648. https://doi.org/10.1039/B205630E
29. Garzón A, Cuevas CA, Ceacero AA (2006) J Chem Phys 125:104305. https://doi.org/10.1063/1.2244556
30. Shannon RJ, Cossou C, Loison JC, Caubet P, Balucani N, Seakins PW, Wakelam V, Hickson KM (2014) RSC Adv 4:26342. https://doi.org/10.1039/C4RA03036B
31. Huang CK, Xu ZF, Nakajima M, Nguyen HMT, Lin MC, Tsuchiya S, Lee YP (2012) J Chem Phys 137:164307. https://doi.org/10.1063/1.4759619
32. Taatjes CA, Christensen LK, Hurley MD, Wallington TJ (1999) J Phys Chem A 103:9805. https://doi.org/10.1021/jp992465l
33. Yasunaga K, Gillespie F, Simmie JM, Curran HJ, Kuraguchi Y, Hoshikawa H, Yamane M, Hidaka Y (2010) J Phys Chem A 114:9098. https://doi.org/10.1021/jp104070a
34. Starik AM, Pelevkin AV, Titova NS (2017) Combust Flame 176:81. http://dx.doi.org/10.1016/j.combustflame.2016.10.005
35. Kaiser EW (2002) J Phys Chem A 106:7, 1256. https://doi.org/10.1021/jp013089j
36. Ludwig W, Brandt B, Friedrichs G, Temps F (2006) J Phys Chem A 110:3330. https://doi.org/10.1021/jp0557464
37. Pan YR, Tang YZ, Sun JY, Sun H, Wang RS (2011) Int J Quantum Chem 111:2922. https://doi.org/10.1155/2018/3036791
38. Zhang HX, Ahonkhai SI, Back MH (1989) Can J Chem 67:1541. https://doi.org/10.1139/v89-235
39. Yan T, Hase WL, Doubleday C (2004) J Chem Phys 120:9253. http://dx.doi.org/10.1063/1.1705574
40. Lee C, Yang W, Parr RG (1988) Phys Rev B 37:785. https://doi.org/10.1103/PhysRevB.37.785
41. Raghunath P, Nghia NT, Lin MC (2014) Adv Quantum Chem 69:253. https://doi.org/10.1016/B978-0-12-800345-9.00007-6
42. Purvis GD III, Bartlett RJ (1982) *J. Chem. Phys. 76*, 1910. https://doi.org/10.1063/1.443164
43. Raghavachari K, Trucks GW, Pople JA, Head-Gordon MA (1989) Chem Phys Lett 157:479–483. https://doi.org/10.1016/S0009-2614(89)87395-6
44. Frisch MJ, Trucks GW, Schlegel HB, Scuseria GE, Robb MA, Cheeseman JR, Scalmani G, Barone V, Mennucci B, Petersson GA, Nakatsuji H, Caricato M, Li X, Hratchian HP, Izmaylov AF, Bloino J, Zheng

G, Sonnenberg JL, Hada M, Ehara M, Toyota K, Fukuda R, Hasegawa J, Ishida M, Nakajima T, Honda Y, Kitao O, Nakai H, Vreven T, Montgomery JA Jr, Peralta JE, Ogliaro F, Bearpark M, Heyd JJ, Brothers E, Kudin KN, Staroverov VN, Keith T, Kobayashi R, Normand J, Raghavachari K, Rendell A, Burant JC, Iyengar SS, Tomasi J, Cossi M, Rega N, Millam JM, Klene M, Knox JE, Cross JB, Bakken V, Adamo C, Jaramillo J, Gomperts R, Stratmann RE, Yazyev O, Austin AJ, Cammi R, Pomelli C, Ochterski JW, Martin RL, Morokuma K, Zakrzewski VG, Voth GA, Salvador P, Dannenberg S, Dapprich AD, Daniels O, Farkas JB, Foresman, Fox (2013) *Gaussian 09, revision D.01*, Gaussian, Inc., Wallingford, CT

45. Eyring H (1935) J Chem Phys 3:107. https://doi.org/10.1063/1.1749604
46. Eckart C (1930) Phys Rev 35:1303. https://doi.org/10.1103/PhysRev.35.1303
47. Barker JR, Ortiz NF, Preses JM, Lohr LL, Maranzana A, Stimac PJ, Nguyen TL, Kumar TJD (2014) MultiWell Programe Suite User Manual, v. 2014.1, University of Michigan, US
48. Jackels CF (1982) J Chem Phys 76:505–515. https://doi.org/10.1063/1.442752
49. Herzberg G (1966) Electronic spectra and electronic structure of polyatomic molecules. Van Nostrand, New York
50. Durig JR, Jin Y, Phan HV, Liu J, Durig DT (2002) Struct Chem 13:1. https://doi.org/10.1023/A:1013410428690
51. Coussan S, Bouteiller Y, Perchard JP, Zheng WQ (1998) J Phys Chem A 102:5789. https://doi.org/10.1021/jp9805961
52. Hellwege KH, Hellwege AM (eds) (1976) Landolt-Bornstein: Group II: atomic and molecular physics volume 7: structure data of free polyatomic molecules. Springer-Verlag, Berlin
53. Huber KP, Herzberg G (1979) Molecular spectra and molecular structure. IV. constants of diatomic molecules. Van Nostrand Reinhold Co.
54. Kuchitsu(K (ed) (1998) Structure of free polyatomic molecules - basic data. Springer, Berlin
55. Gurvich LV, Veyts IV, Alcock CB (1989) Thermodynamic properties of individual substances, fouth edition. Hemisphere Pub. Co., New York
56. Ruscic B, Boggs JE, Burcat A, Csaszar AG, Demaison J, Janoschek R, Martin JML, Morton ML, Rossi MJ, Stanton JF, Szalay PG, Westmoreland PR, Zabel F, Berces T (2005) J Phys Chem Ref Data 34:573. https://doi.org/10.1063/1.1724828
57. Cox JD, Wagman DD, Medvedev VA (1989)CODATA key values for thermodynamics, Hemisphere, New York
58. Frenkel M, Marsh KN, Wilhoit RC, Kabo GJ, Roganov GN (1994) Thermodynamics of organic compounds in the gas state, Thermodynamics research center, College Station, TX
59. Berkowitz J, Ellison GB, Gutman D (1994) J Phys Chem 98:2744. https://doi.org/10.1021/j100062a009

Figures

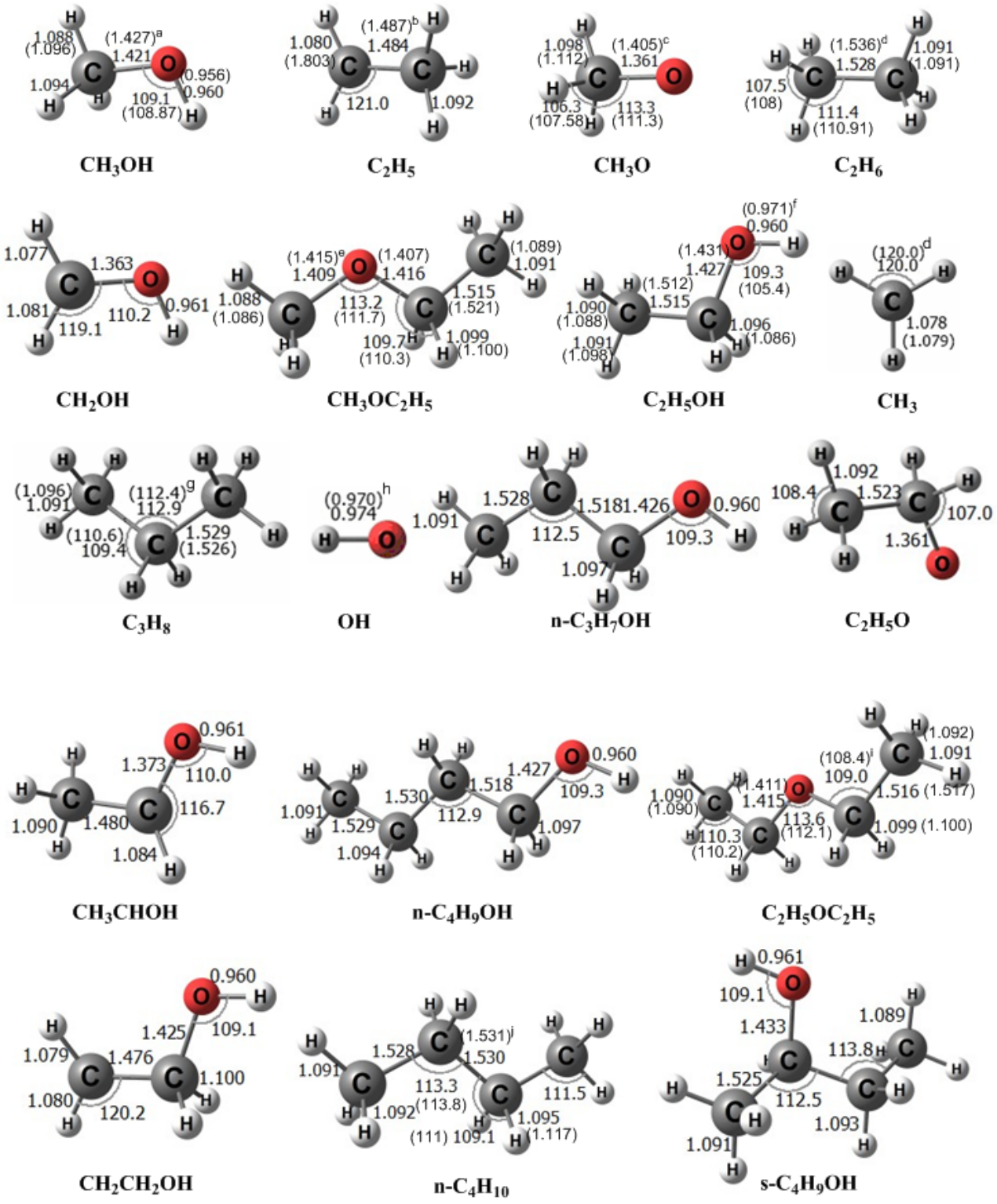

Figure 1

Geometries of the reactants and products related to the C_2H_5 + $C_nH_{2n+1}OH$ (n = 1, 2) reactions. [a-j]The values in the parenthesis are from the literature. [10,36,47-53]

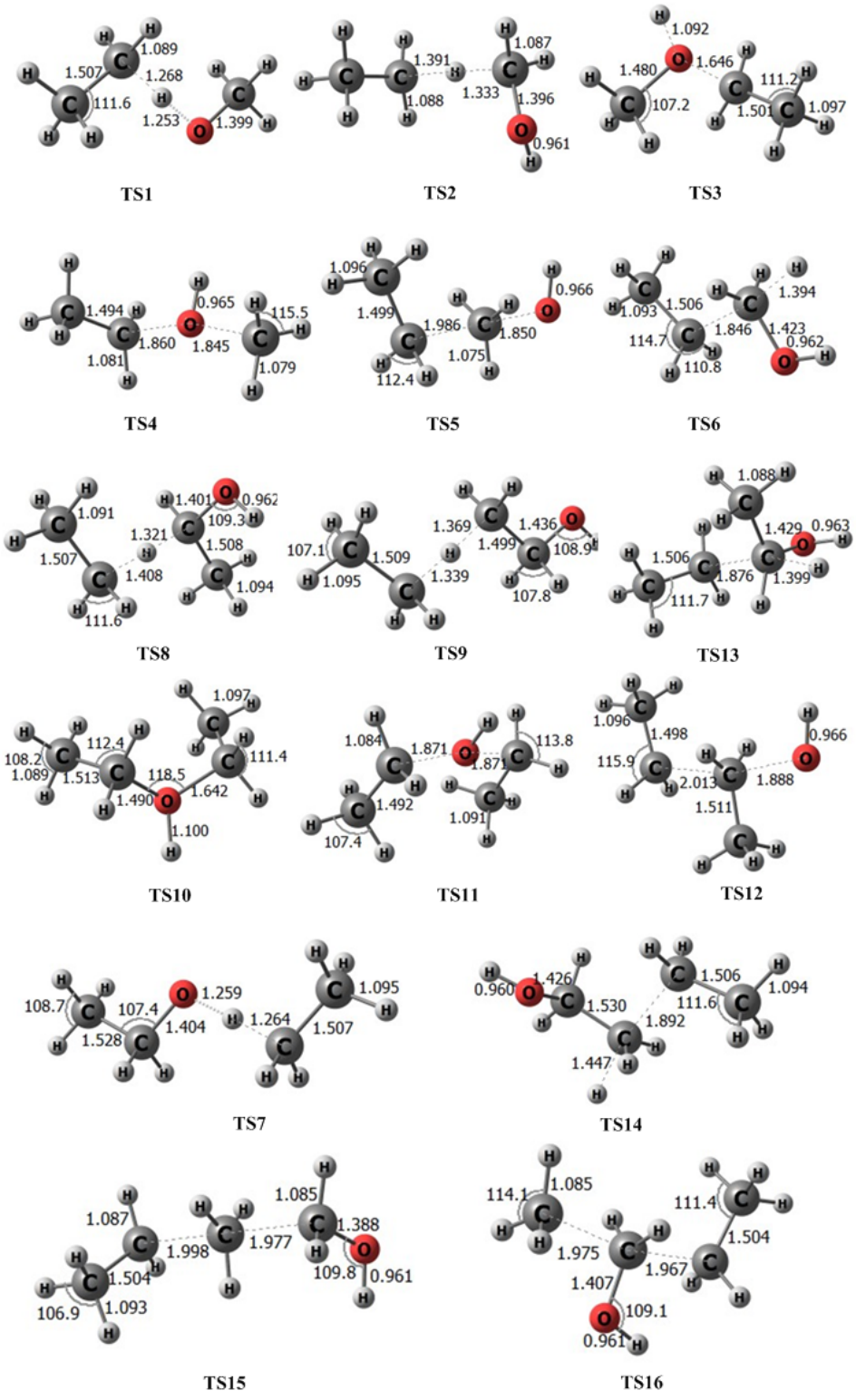

Figure 2

Geometries of the transition states related to the C_2H_5 + $C_nH_{2n+1}OH$ (n = 1, 2) reactions.

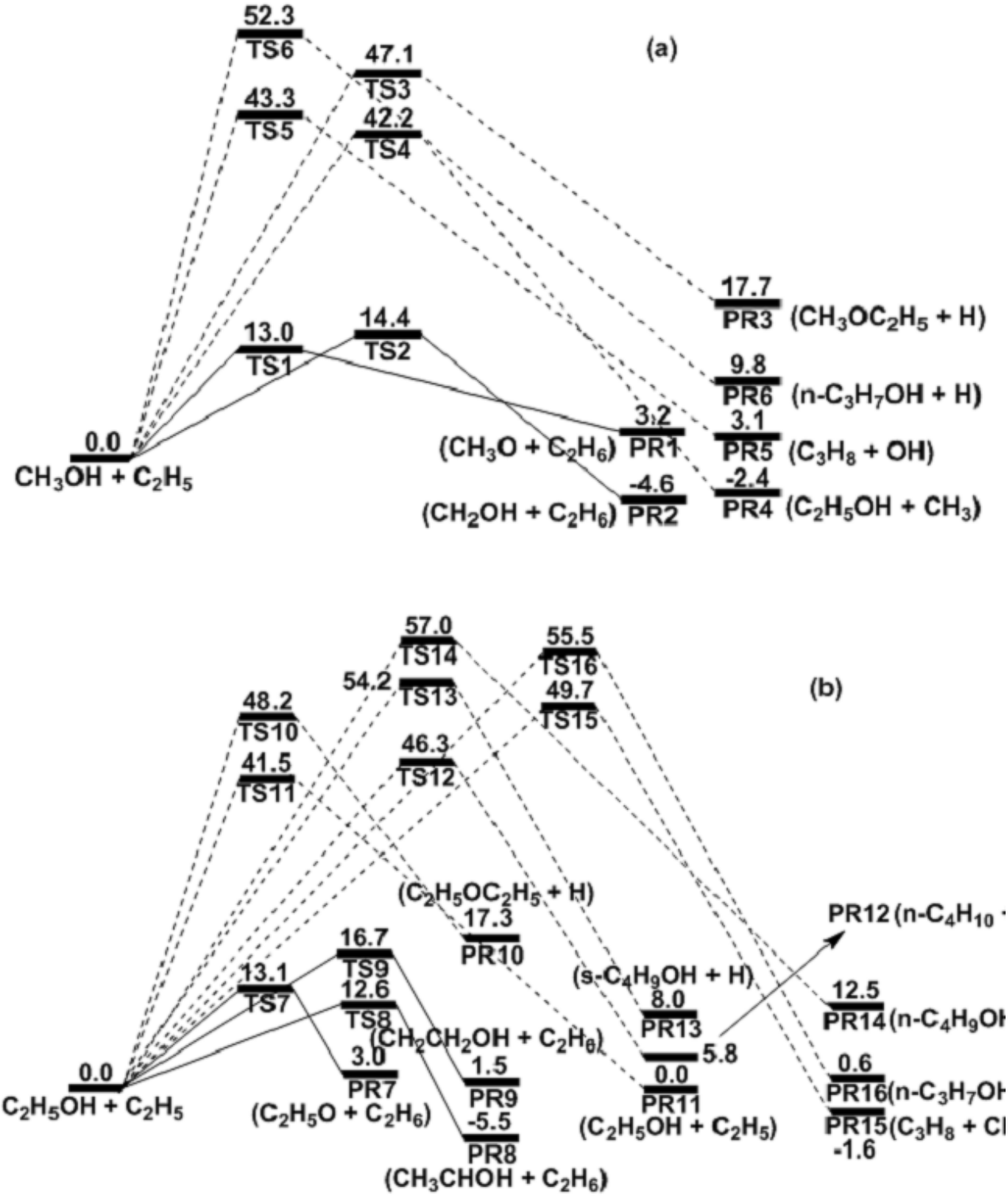

Figure 3

Potential energy profiles for the C_2H_5 + $C_nH_{2n+1}OH$ (n = 1, 2) reactions.

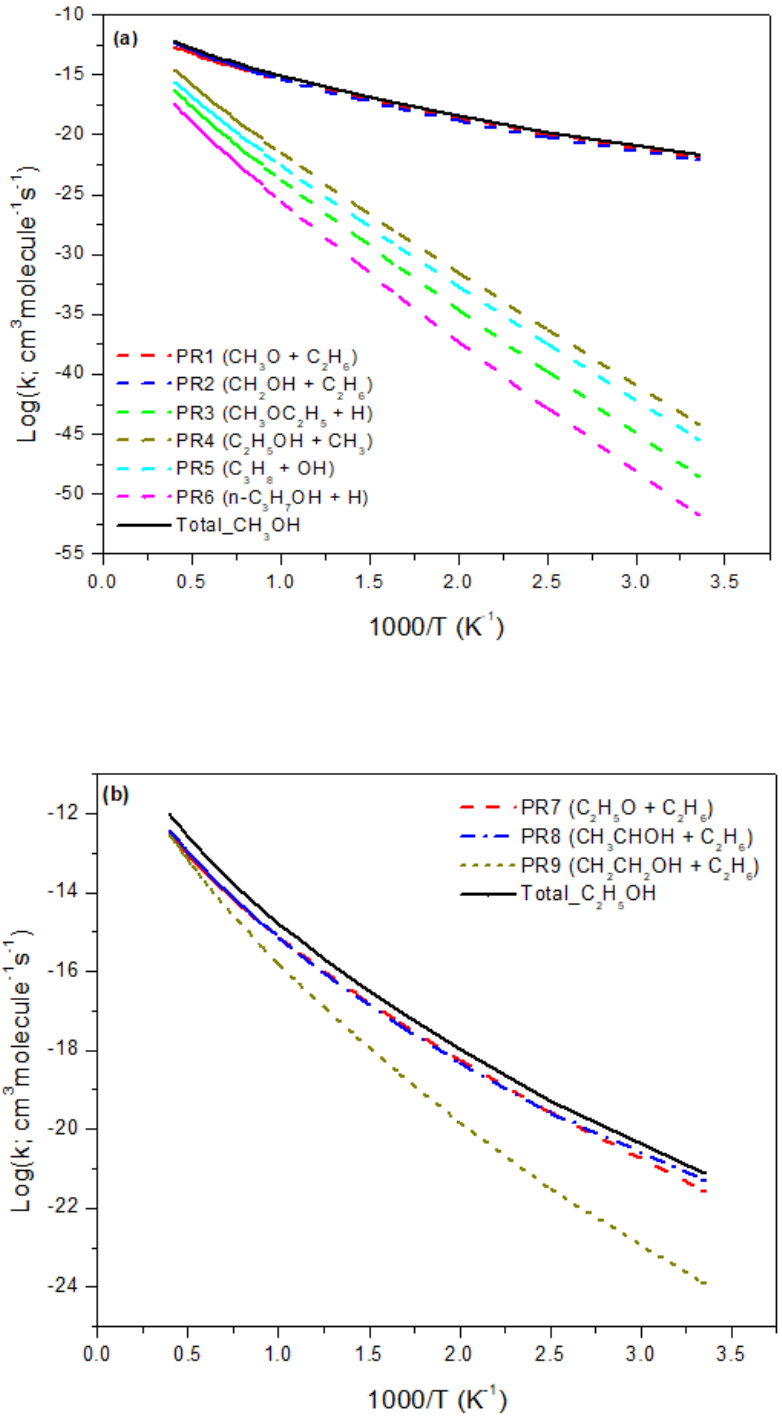

Figure 4

Arrhenius plots of bimolecular reactions of the C_2H_5 + $C_nH_{2n+1}OH$ (n = 1, 2) reactions.

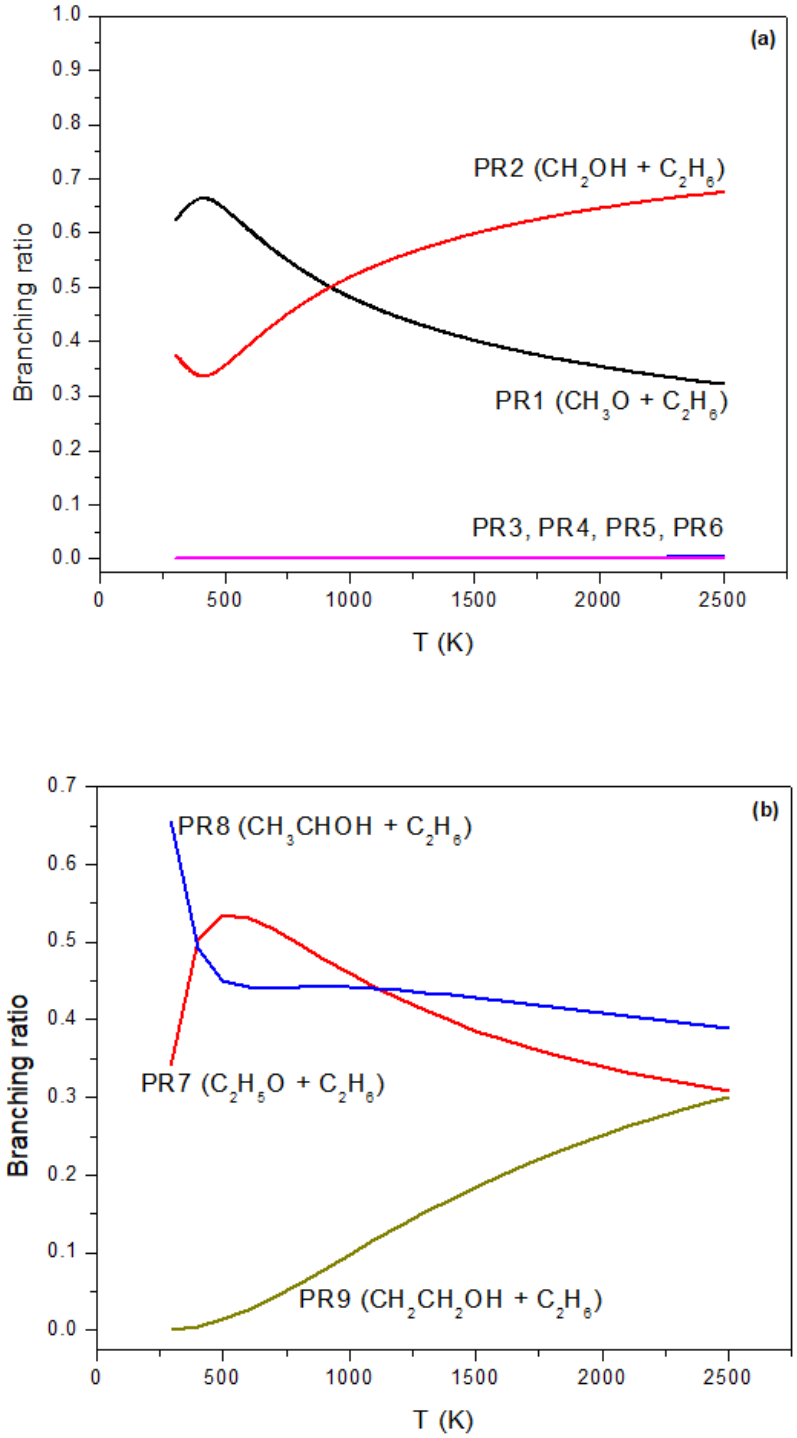

Figure 5

Branching ratios for the C_2H_5 + $C_nH_{2n+1}OH$ (n = 1, 2) reactions.

Supplementary Files

This is a list of supplementary files associated with this preprint. Click to download.

- SIC2H5ancol.doc